A flexible, high-performance magnetoelectric heterostructure of (001) oriented Pb(Zr_{0.52}Ti_{0.48})O₃ film grown on Ni foil

Cite as: APL Mater. 5, 096111 (2017); https://doi.org/10.1063/1.4993239 Submitted: 28 June 2017 . Accepted: 23 August 2017 . Published Online: 28 September 2017

Haribabu Palneedi, Hong Goo Yeo, Geon-Tae Hwang, Venkateswarlu Annapureddy, Jong-Woo Kim, Jong-Jin Choi, Susan Trolier-McKinstry, and Jungho Ryu









ARTICLES YOU MAY BE INTERESTED IN

Comprehensive biocompatibility of nontoxic and high-output flexible energy harvester using lead-free piezoceramic thin film

APL Materials 5, 074102 (2017); https://doi.org/10.1063/1.4976803

High-temperature crystallized thin-film PZT on thin polyimide substrates

Journal of Applied Physics 122, 164103 (2017); https://doi.org/10.1063/1.4990052

Multiferroic magnetoelectric composites: Historical perspective, status, and future directions

Journal of Applied Physics 103, 031101 (2008); https://doi.org/10.1063/1.2836410







A flexible, high-performance magnetoelectric heterostructure of (001) oriented Pb(Zr_{0.52}Ti_{0.48})O₃ film grown on Ni foil

Haribabu Palneedi, 1,a Hong Goo Yeo, 2,a Geon-Tae Hwang, 1 Venkateswarlu Annapureddy, 1 Jong-Woo Kim, 1 Jong-Jin Choi, 1 Susan Trolier-McKinstry, 2,b and Jungho Ryu1,b

¹Functional Ceramics Group, Korea Institute of Materials Science, Changwon 51508, South Korea

²Materials Research Institute, The Pennsylvania State University, University Park, Pennsylvania 16802, USA

(Received 28 June 2017; accepted 23 August 2017; published online 28 September 2017)

In this study, a flexible magnetoelectric (ME) heterostructure of PZT/Ni was fabricated by depositing a (001) oriented Pb(Zr_{0.52}Ti_{0.48})O₃ (PZT) film on a thin, flexible Ni foil buffered with LaNiO₃/HfO₂. Excellent ferroelectric properties and large ME voltage coefficient of 3.2 V/cm·Oe were realized from the PZT/Ni heterostructure. The PZT/Ni composite's high performance was attributed to strong texturing of the PZT film, coupled with the compressive stress in the piezoelectric film. Besides, reduced substrate clamping in the PZT film due to the film on the foil structure and strong interfacial bonding in the PZT/LaNiO₃/HfO₂/Ni heterostructure could also have contributed to the high ME performance of PZT/Ni. © 2017 Author(s). All article content, except where otherwise noted, is licensed under a Creative Commons Attribution (CC BY) license (http://creativecommons.org/licenses/by/4.0/). https://doi.org/10.1063/1.4993239

Recent research efforts have focused on designing metal-based micro-electro-mechanical systems (M-MEMSs) by growing piezoelectric ceramic films on flexible base metal foils. The low cost of these foils, coupled with their ready availability, makes them particularly useful in the development of embedded capacitors, energy harvesting devices, and wearable electronics. ¹⁻⁵ Advantages of these foils include the possibility of large area fabrication and on demand design adaptivity. Additionally, their high fracture strength provides a superior alternative to brittle, rigid Si substrates when they are stressed by large deformations and impacts. The coupling of functional metal substrates with piezoelectric films allows for the development of multifunctional devices. Interestingly, magnetoelectric (ME) film heterostructures involve a similar design, in which a piezoelectric film is deposited on a magnetostrictive metallic substrate. These ME composites with multifunctionality can be used in many ways. For example, the ME heterostructure could function as a dual-phase (piezoelectric as well as magnetoelectric) sensor and energy harvester. The film on foil structured ME based devices could operate at low resonance frequencies with high sensitivity. Such devices could sense biomagnetic signals with high spatial resolution and scavenge energy from ambient vibrations, human body motions, and stray magnetic fields.^{5–7} ME composites have potential applications in magnetic sensors, transducers, filters, oscillators, phase shifters, data storage elements, and energy harvesting systems.8-11

Among the piezoelectric/magnetostrictive constituents available for fabricating an ME heterostructure, the combination of Pb(Zr,Ti)O₃ (PZT) and Ni is an attractive option, as PZT has high piezoelectric response and Ni is an inexpensive and widely available magnetostrictive base metal. Further, the similar mechanical impedances of PZT (25–30 MRayl) and Ni (27 MRayl) should enable

^bAuthors to whom correspondence should be addressed: set1@psu.edu and jhryu@kims.re.kr



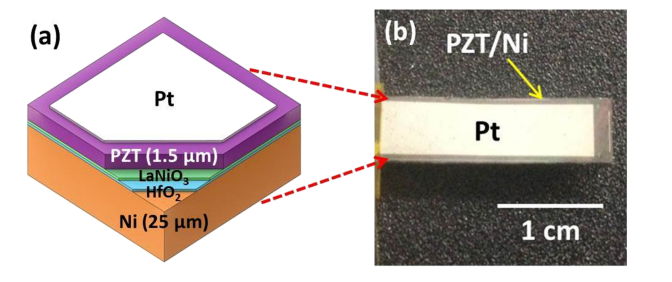
^aH. Palneedi and H. G. Yeo contributed equally to this work.

efficient strain transfer across the PZT/Ni interface. This, in turn, should produce strong ME coupling in PZT/Ni composites. 12,13 The performance of an ME composite, quantified in terms of the ME voltage coefficient (α_{ME}), depends mainly on the efficiency of coupling between the magnetic and electric domains of the magnetostrictive and piezoelectric phases, respectively. Although some previous studies have reported the development of PZT/Ni film-based ME composites, it has been challenging to achieve an appreciable ME output. 13-15 This can be attributed to the processing issues raised by the thermodynamic incompatibility between PZT and Ni. If no passivation layers are utilized during PZT film crystallization, the high temperatures required cause oxidation of Ni and interfacial chemical reactions between PZT and Ni; these complicate the strain transfer and impair the ME coupling. Employment of buffer layers between the PZT and Ni can improve the situation to some extent. Gupta et al. measured α_{ME} of 0.22 V/cm·Oe from a rapid thermal annealed (RTA) PZT film grown on the Ni foil. ¹⁵ Feng *et al.* observed α_{ME} of 0.772 V/cm·Oe in the PZT/Pt/Ni multiferroic film heterostructure at an optimum Pt-thickness of 30 nm. ¹⁴ Kambale *et al.* reported α_{ME} of 1 V/cm·Oe in a PZT film deposited on Ni with an LNO buffer layer between them.¹³ Comparison of the measured α_{ME} values of PZT/Ni film composites with the ideally obtainable ones suggest that there is room for improvement in ME coupling of PZT/Ni.¹⁴

It is well known that the piezoelectric response of ceramics can be tailored by tuning their composition (via suitable stoichiometry and doping) and microstructural design (via grain and domain engineering). $^{16-19}$ Crystallographically oriented piezoelectric ceramic films have been shown to demonstrate better piezoelectric performance than their randomly oriented counterparts. $^{20-23}$ Although there have been some efforts to synthesize textured PZT films on magnetostrictive oxide substrates, which showed poor ME outputs, fabrication of ME composites with oriented PZT films on Ni has been rarely reported. $^{24-27}$ In this context, the present work is directed towards development of a high-performance PZT/Ni magnetoelectric film heterostructure. The large α_{ME} of 3.2 V/cm-Oe obtained from a (001) oriented PZT film on the Ni foil is found be the best reported to date for ME film composites based on either PZT/Ni or textured PZT films on magnetostrictive oxide substrates.

A schematic of the PZT/Ni heterostructure and photos of the flexible sample are shown in Fig. 1. The in-plane dimensions of the sample are $21.5 \times 6.5 \text{ mm}^2$. The PZT/Ni sample was prepared following the procedure described elsewhere⁴ and in the supplementary material. A 1.5 μ m-thick PZT film was deposited on a 25 μ m-thick, Ni (Alfa Aesar, 99.99%) foil. The PZT film was corona poled at 130 °C for 20 min using DC electric voltages (7-12 kV), with the needle to sample distance kept at 30 mm.

The crystallographic structure of the PZT film was investigated using an X-ray diffractometer (XRD, D/Max 2200, Rigaku, Japan). The cross-sectional features of the PZT film were observed using a field emission scanning electron microscope (FESEM, Leo 1530, Zeiss, Germany) and a transmission electron microscope (TEM, JSM-2100F, JEOL, Japan). Elemental distributions across the PZT/LNO/HfO₂/Ni heterostructure were examined by Energy-dispersive X-ray spectroscopy (EDS) on the TEM, using the sample milled by the focused ion beam technique. Dielectric properties of the PZT film were measured by an impedance analyzer (HP4294A, Agilent, USA) while its polarization hysteresis behavior was evaluated by a ferroelectric test system (Precision LC II, Radiant,



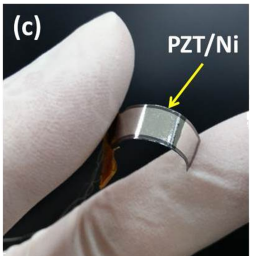


FIG. 1. (a) Schematic of the ME heterostructure of PZT film with LNO and HfO_2 buffer layers on Ni. [(b) and (c)] Photos of the flexible PZT/Ni composite.

USA). The ME voltage signal from the PZT/Ni sample was recorded using a lock-in amplifier (SR-850, Stanford Research Systems, USA) as a function of the applied magnetic field. The off-resonance (f = 1 kHz) ME coefficient of the PZT/Ni composite was measured in the thickness direction by subjecting the sample to superimposed AC ($H_{ac} = 1 \text{ Oe}$) and DC (H_{bias}) magnetic fields along the in-plane direction. The in-plane magnetization of the as-received Ni foil and the PZT/Ni composite was evaluated using a physical property measurement system (PPMS, Quantum Design, USA).

The XRD pattern of the PZT film deposited on the LNO/HfO₂ buffered Ni foil is shown in Fig. 2(a). The film exhibits a strong (001) grain orientation without any secondary phase. This suggests successful templating from the (100) oriented LNO seed layer. The cross-sectional FESEM image of the PZT film [Fig. 2(b)] depicts the columnar growth of the PZT grains. This is also evident from the cross-sectional TEM image [Fig. 2(c)]; columnar grains with clear crystallization interfaces are apparent, where the PZT columns extended across the thickness of the layer. The crystallization interfaces are a consequence of multiple spin-coating and RTA steps which induce direct epitaxial growth of a new layer on top of a pre-existing crystallized layer. 25,27

Mechanical characterization of the PZT/Ni heterostructure was conducted through bending test of the sample to estimate its structural integrity. The quality of interfacial bonding was gauged by observing the surface microstructure of the PZT film under bending strains of 0.19% and 0.29% applied to the PZT/Ni composite (see Fig. S1 of the supplementary material). The microstructure of the PZT film remained unchanged and the bending strain did not cause any cracking or delamination in the film. This result serves as evidence for the strong interfacial bonding of the PZT film via the HfO₂/LNO buffer layer to the Ni foil, which would ensure efficient strain transfer and ME coupling between PZT and Ni.

The frequency (f) dependent dielectric constant (ε_r) and loss tangent ($\tan \delta$) of the PZT film on the Ni foil are shown in Fig. 3(a). At f=1 kHz, the values of ε_r and $\tan \delta$ were 470 and 0.045, respectively. Clearly, the PZT film has a significantly lower dielectric constant than that reported for (100) oriented PZT deposited on Si (>1000). ¹⁶ As described before, the low permittivity of the film is attributed to the large c-domain population in the PZT film. ²⁸ The ferroelectric polarization curves of the PZT film are presented in Fig. 3(b). Under an applied voltage of 80 V (~530 kV/cm), the curves display a well-saturated square hysteresis loop with a remanent polarization (P_r) ~ 35 μ C/cm² and a coercive field (E_c) ~ 50 kV/cm. The square hysteresis loop and remanent polarization of the (001)

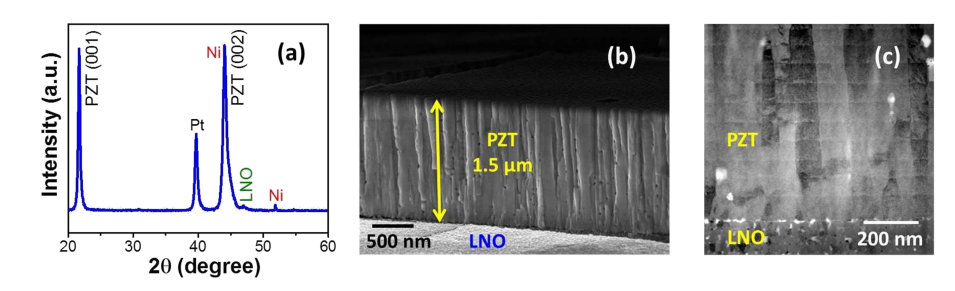


FIG. 2. (a) XRD pattern of the PZT film on LNO/HfO $_2$ /Ni. [(b) and (c)] Cross-sectional images of the PZT film obtained by FESEM and TEM, respectively.

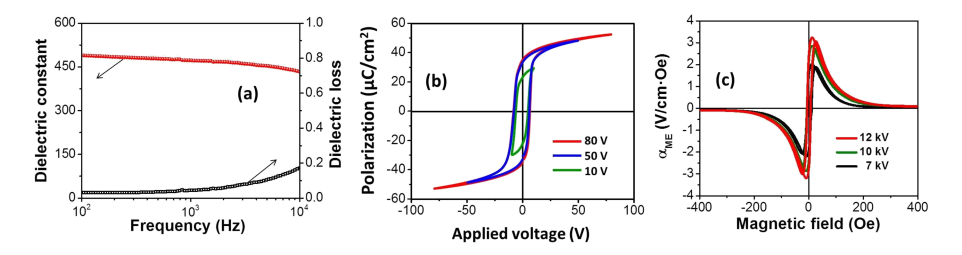


FIG. 3. [(a) and (b)] Dielectric and ferroelectric properties of PZT film on the Ni foil, respectively, and (c) magnetoelectric behavior of the PZT/Ni heterostructure with different applied DC voltages during corona poling.

PZT film on the flexible Ni foil are observed to be much better compared to those reported for the (001) PZT films deposited on rigid magnetostrictive oxide substrates and suggest a large piezoelectric response. The large c-domain population in the PZT film on Ni could be due to a combination of the compressive stress induced by the thermal expansion mismatch between PZT and Ni and the relaxation of stress by bending of the thin foil structure. 4,5,22,29

The ME response of the PZT/Ni composite corona poled at different DC voltages is shown in Fig. 3(c). An optimized maximum α_{ME} of 3.2 V/cm·Oe was obtained at $H_{dc}=10$ Oe, after corona poling under 12 kV at 130 °C for 20 min. Above this DC field, the PZT film cracked and delaminated from the Ni foil. A comparison of the α_{ME} values of various reported ME composites relevant to this work is shown in Table S1 of the supplementary material. $^{13-15,24-27,30}$ The α_{ME} obtained from the (001) oriented PZT film on the Ni foil significantly outperforms that of all the ME film composites based on either PZT/Ni or textured PZT films deposited on magnetostrictive oxide substrates. The high piezoelectric response and the low dielectric constant, due to the strong texturing of the PZT grains and their domain state, presumably contributed to the larger ME output, since $\alpha_{ME} \propto g_{ij}$ (= d_{ij}/ϵ_{ij}), where ϵ_{ij} is dielectric permittivity and g_{ij} and d_{ij} are piezoelectric voltage and charge coefficients, respectively. 31,32 The low permittivity achieved in predominantly c-domain films is useful in increasing the α_{ME} value. It is also believed that the reduced substrate clamping in the PZT film due to the film on the foil structure and the strong interfacial bonding of the PZT/LNO/HfO₂/Ni heterostructure should allow for better strain transfer and in turn stronger ME coupling between PZT and Ni.

The α_{ME} of the PZT/Ni cantilever structure was measured by applying the magnetic field (H_{bias}) along its length (l_c) and width (w_c) directions as depicted in Fig. 4(a). The value of α_{ME} is found to be higher (3.2 V/cm·Oe) when H_{bias}/Il_c compared to that (2 V/cm·Oe) for $H_{bias}/I/w_c$ [Fig. 4(b)]. The value of the ME charge coefficient (α_{mc}) of the PZT/Ni heterostructure is calculated using the relation: $\alpha_{mc} = C \ t \ \alpha_{ME}$, where C is the capacitance (387.5 pF) and t is the thickness (1.5 μ m) of the PZT film. 33,34 The estimated values of α_{mc} of the PZT/Ni composite for the cases of H_{bias}/Il_c and $H_{bias}/I/w_c$ are 0.186 pC/Oe and 0.124 pC/Oe, respectively. These directional variations in ME response of PZT/Ni may be related to the demagnetization effect and the resultant differential magnetic flux distribution in the Ni foil. The effective magnetic field (H_{eff}) and magnetic induction (B_{eff}) in the magnetic phase are influenced by the demagnetizing field (H_d) and the applied magnetic field (H_{bias}) according to $^{35-37}$

$$H_{eff} = H_{bias} - H_d = H_{bias} - MN_d, \tag{1}$$

$$B_{eff} = \mu_0 \left(H_{eff} + M \right) = \mu_0 \left(H_{bias} + M \right) - \mu_0 M N_d, \tag{2}$$

where M is the magnetization, N_d is the demagnetization factor, and μ_0 is the magnetic permeability of free space. Smaller demagnetization results in a stronger effective magnetic induction in the magnetic phase and thus larger ME coupling in the composite. For a finite non-spherical ferromagnet, the demagnetization factor is dependent on its structural parameters. The relation between the ME coefficient and demagnetization factor of a rectangular ME laminate can be simply expressed as

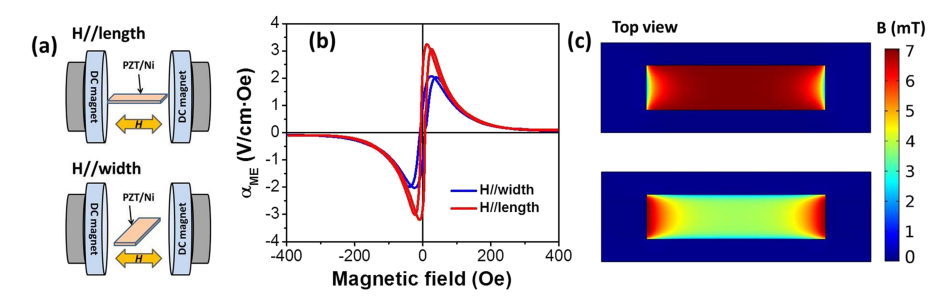


FIG. 4. (a) Schematics of the ME measurement of the PZT/Ni sample subjected to a DC bias in its length and width directions, (b) H_{bias} dependence of α_{ME} for the PZT/Ni composite, and (c) FEM results of in-plane magnetic flux density distribution along the center plane of the Ni foil in the condition of H//length (upper image) and H//width (lower image).

 $\alpha_{ME} \propto (1 + \beta)/N_d$, where $\beta \approx \sqrt{N_l/N_w}$ is the magnetostriction factor, $N_l \approx 2t\pi/l$ is the demagnetization factor along the length, and $N_w \approx 2t\pi/w$ is the demagnetization factor along the width of the rectangular magnetostrictive layer. The lower value of N_l than N_w will lead to a higher magnitude of α_{ME} of the PZT/Ni cantilever along its length compared to that in its width direction.

To understand further, the magnetic flux density distribution in the Ni foil was simulated using a finite element model (FEM, COMSOL Multiphysics 5.2). In this model, it was assumed that a rectangular Ni foil, with dimensions similar to those used in the experiments and a relative permeability of 600, was placed in air and subjected to a magnetic field of 1 Oe in its length and width directions. For the simulation, a magnetostatic insulating boundary condition was applied around Ni, which was meshed with a maximum element size of 1 μ m. Figure 4(c) displays the simulated magnetic flux density distribution in the Ni foil for the magnetic field applied along its length and width. It is evident that the Ni foil exhibits a much stronger magnetic induction when H_{bias}/II_{Ni} compared to that for $H_{bias}/I/w_{Ni}$. Moreover, the highest B_{eff} is concentrated towards the center of Ni in the former case, while it is concentrated towards the edges of the Ni foil in the later case. These can be due to the corresponding changes in H_d , N_d , and H_{eff} in both the H_{bias} applied directions. The differences in intensities of B_{eff} may have resulted in the varied magnitudes of α_{ME} of the PZT/Ni composite along its length and width.

The magnetization behavior of a pure Ni foil and the PZT/Ni composite are compared in Fig. 5. There are minor changes in the magnitude of the coercive field (H_c) and magnetization (M) between the two samples. It has been reported that stress facilitates magnetization when $\sigma \lambda > 0$, where σ is stress and λ is magnetostriction. As discussed above, the larger thermal expansion of Ni, relative to PZT, induces compressive stress in the PZT film on cooling. Since λ of Ni (-40 ppm) is negative, the tensile stress in the Ni foil is expected to have caused the decrease in magnetization of PZT/Ni. Besides, the NiO layer formed on Ni (see Fig. S2 of the supplementary material) too might have contributed to the decrease in magnetization of the composite. Quantification of the effects of the stress in the Ni foil and the NiO layer formation on ME coupling of PZT/Ni needs further evaluation. It can be inferred that there is a possibility to scale up the ME output by controlling the stress in the Ni foil (by depositing the PZT film on both sides of Ni and by connecting the upper and lower PZT layers in series) and avoiding its oxidation (through optimization of HfO₂ layer thickness).

In summary, a high-performance composite material was developed from a flexible ME heterostructure of (001) oriented PZT film grown on a thin, flexible Ni foil. The PZT/Ni composite exhibited a large ME voltage coefficient of 3.2 V/cm·Oe and superior ferroelectric properties, which were attributed to the strong texturing of the PZT film and the compressive stress in the piezoelectric film. The high performance of PZT/Ni could have also been derived from reduced substrate clamping in the PZT film due to the film on the foil structure and strong interfacial bonding in the PZT/LNO/HfO₂/Ni heterostructure. The PZT/Ni composite outperformed other known ME film composites based on PZT/Ni as well as those composites of textured PZT films deposited on magnetostrictive oxide substrates. The high-performance ME film heterostructure is promising for metal-based MEMS devices with potential applications in embedded capacitors, energy harvesting systems, magnetic sensors, and wearable electronics.

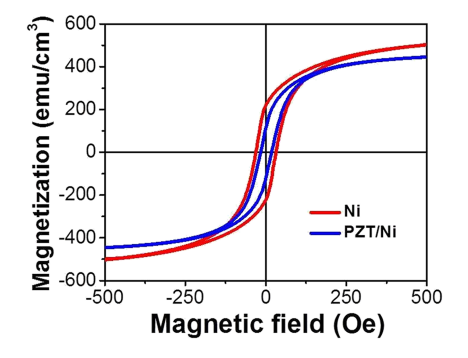


FIG. 5. Magnetization hysteresis loops of the as-received Ni foil and the PZT/Ni composite.

See supplementary material for fabrication of the PZT/Ni ME heterostructure, its mechanical and microstructural characterization, and comparison of its ME performance with the literature reported results.

This research work was supported by the National Research Foundation of Korea (Grant No. NRF-2016R1A2B4011663), Korea Institute of Materials Science (KIMS) internal R&D program (Grant Nos. PNK5061 and PNK 5082), the NSF ASSIST ERC (Grant No. EEC-1160483), and the U.S. Office of Naval Research Global (Grant No. N62909-16-1-2135).

```
<sup>1</sup> J.-P. Maria, K. Cheek, S. Streiffer, S.-H. Kim, G. Dunn, and A. I. Kingon, J. Am. Ceram. Soc. 84, 2436 (2001).
```

- ² A. I. Kingon and S. Srinivasan, Nat. Mater. 4, 233 (2005).
- ³ C. T. Shelton and B. J. Gibbons, J. Am. Ceram. Soc. **94**, 3223 (2011).
- ⁴ H. G. Yeo and S. Trolier-McKinstry, J. Appl. Phys. **116**, 014105 (2014).
- ⁵ H. G. Yeo, X. Ma, C. Rahn, and S. Trolier-McKinstry, Adv. Funct. Mater. 26, 5940 (2016).
- ⁶ R. Jahns, A. Piorra, E. Lage, C. Kirchhof, D. Meyners, J. L. Gugat, M. Krantz, M. Gerken, R. Knöchel, and E. Quandt, J. Am. Ceram. Soc. **96**, 1673 (2013).
- ⁷ S. Lee, S.-H. Bae, L. Lin, Y. Yang, C. Park, S.-W. Kim, S. N. Cha, H. Kim, Y. J. Park, and Z. L. Wang, Adv. Funct. Mater. **23**, 2445 (2013).
- ⁸ J. Ryu, S. Priya, K. Uchino, and H.-E. Kim, J. Electroceram. **8**, 107 (2002).
- ⁹ Y. Zhou, J.-W. Kim, S. Dong, S. Priya, J. Wang, and J. Ryu, "Applications of multiferroic magnetoelectric composites," in *Multiferroic Materials Properties, Techniques, and Applications*, edited by J. Wang (CRC Press, Boca Raton, FL, USA, 2017), Chap. 8.
- ¹⁰ V. Annapureddy, M. Kim, H. Palneedi, H.-Y. Lee, S.-Y. Choi, W.-H. Yoon, D.-S. Park, J.-J. Choi, B.-D. Hahn, C.-W. Ahn, J.-W. Kim, D.-Y. Jeong, and J. Ryu, Adv. Energy Mater. 6, 1601244 (2016).
- ¹¹ J. Ryu, J.-E. Kang, Y. Zhou, S.-Y. Choi, W.-H. Yoon, D.-S. Park, J.-J. Choi, B.-D. Hahn, C.-W. Ahn, J.-W. Kim, Y.-D. Kim, S. Priya, S. Y. Lee, S. Jeong, and D.-Y. Jeong, Energy Environ. Sci. 8, 2402 (2015).
- ¹² J. G. Wan, J.-M. Liu, H. L. W. Chand, C. L. Choy, G. H. Wang, and C. W. Nan, J. Appl. Phys. **93**, 9916 (2003).
- ¹³ R. C. Kambale, J. Ryu, D. R. Patil, Y. S. Chai, K. H. Kim, W.-H. Yoon, D.-Y. Jeong, D.-S. Park, J.-W. Kim, J.-J. Choi, and C.-W. Ahn, J. Phys. D: Appl. Phys. 46, 092002 (2013).
- ¹⁴ M. Feng, J.-J. Wang, J.-M. Hu, J. Wang, J. Ma, H.-B. Li, Y. Shen, Y.-H. Lin, L.-Q. Chen, and C.-W. Nan, Appl. Phys. Lett. **106**, 072901 (2015).
- ¹⁵ R. Gupta, M. Tomar, V. Gupta, Y. Zhou, A. Chopra, S. Priya, A. S. Bhalla, and R. Guo, Energy Harvesting Syst. 3, 181 (2016).
- ¹⁶ F. Calame and P. Muralt, Appl. Phys. Lett. **90**, 062907 (2007).
- ¹⁷ D. Damjanovic, Rep. Prog. Phys. **61**, 1267 (1998).
- ¹⁸ S. Trolier-McKinstry, F. Griggio, C. Yaeger, P. Jousse, D. Zhao, S. S. N. Bharadwaja, T. N. Jackson, S. Jesse, S. V. Kalinin, and K. Wasa, IEEE Trans. Ultrason., Ferroelectr., Freq. Control 58, 1782 (2011).
- ¹⁹ C. B. Yeager, Y. Ehara, N. Oshima, H. Funakubo, and S. Trolier-McKinstry, J. Appl. Phys. 116, 104907 (2014).
- ²⁰ N. Ledermann, P. Muralt, J. Baborowski, S. Gentil, K. Mukati, M. Cantoni, A. Seifert, and N. Setter, Sens. Actuators, A 105, 162 (2003).
- ²¹ S. Yokoyama, Y. Honda, H. Morioka, S. Okamoto, H. Funakubo, T. Iijima, H. Matsuda, K. Saito, T. Yamamoto, H. Okino, O. Sakata, and S. Kimura, J. Appl. Phys. 98, 094106 (2005).
- ²² S. Trolier-McKinstry and P. Muralt, "Thin film piezoelectrics for MEMS," in *Electroceramic Based MEMS: Fabrication-Technology and Applications*, edited by N. Setter (Springer, New York, 2005), Chap. 10, p. 199.
- ²³ V. Annapureddy, J.-J. Choi, J.-W. Kim, B.-D. Hahn, C.-W. Ahn, and J. Ryu, J. Korean Phys. Soc. **68**, 1390 (2016).
- ²⁴ S. Ryu, J. H. Park, and H. M. Jang, Appl. Phys. Lett. **91**, 142910 (2007).
- ²⁵ R. Lin, T.-B. Wu, and Y.-H. Chu, Scr. Mater. **59**, 897 (2008).
- ²⁶ Z. Duan, X. Shi, Y. Cui, Y. Wan, Z. Lu, and G. Zhao, J. Alloys Compd. **698**, 276 (2017).
- ²⁷ K. Tahmasebi, A. Barzegar, J. Ding, T. S. Herng, A. Huang, and S. Shannigrahi, Mater. Des. 32, 2370 (2011).
- ²⁸ C. B. Yeager and S. Trolier-McKinstry, J. Appl. Phys. **112**, 074107 (2012).
- ²⁹ G. Han, J. Ryu, W.-H. Yoon, J.-J. Choi, B.-D. Hahn, J.-W. Kim, D.-S. Park, C.-W. Ahn, S. Priya, and D.-Y. Jeong, J. Appl. Phys. 110, 124101 (2011).
- ³⁰ C.-S. Park, A. Khachaturyan, and S. Priya, Appl. Phys. Lett. **100**, 192904 (2012).
- ³¹ S. Dong, J. Zhai, Z. Xing, J. Li, and D. Viehland, Appl. Phys. Lett. **91**, 022915 (2007).
- ³² J. Ryu, A. V. Carazo, K. Uchino, and H.-E. Kim, Jpn. J. Appl. Phys., Part 1 40, 4948 (2001).
- ³³ Z. Xing, "Magnetoelectric device and the measuring unit," Ph.D. thesis, Virginia Tech, USA, 2009.
- ³⁴ J. T. Evans, S. P. Chapman, S. T. Smith, B. C. Howard, and A. Gallegos, "Measuring magnetoelectric and magnetopiezoelectric effects," in *Proceedings of ISAF-ECAPD-PFM*, Aveiro, Portugal, 9–13 July 2012 (IEEE, 2012).
- ³⁵ Y. Zhou, S. C. Yang, D. J. Apo, D. Maurya, and S. Priya, Appl. Phys. Lett. **101**, 232905 (2012).
- ³⁶ Y. Zhou and S. Priya, J. Appl. Phys. **115**, 104107 (2014).
- ³⁷ Z. Chu, H. Shi, W. Shi, G. Liu, J. Wu, J. Yang, and S. Dong, Adv. Mater. **29**, 1606022 (2017).
- ³⁸ D. A. Pan, J. Lu, Y. Bai, W. Y. Chu, and L. J. Qiao, Chin. Sci. Bull. **53**, 2124 (2008).
- ³⁹ R. C. Kambale, J.-E. Kang, W.-H. Yoon, D.-S. Park, J.-J. Choi, C.-W. Ahn, J.-W. Kim, B.-D. Hahn, D.-Y. Jeong, Y.-D. Kim, S. Dong, and J. Ryu, Energy Harvesting Syst. 1, 3 (2014).
- ⁴⁰ J. Wang, Z. Li, J. Wang, H. He, and C. Nan, J. Appl. Phys. **117**, 044101 (2015).